Письма в ЭЧАЯ. А. 2011. Т. 8, № 8. С. 61–71

HAGEDORN STATES AND THERMALIZATION

J. Noronha-Hostler [a, b, c], *C. Greiner* [b]

[a] Frankfurt Institute for Advanced Studies (FIAS), Frankfurt am Main, Germany

[b] Institut für Theoretische Physik, Johann Wolfgang Goethe-Universität, Frankfurt am Main, Germany

[c] Helmholtz Research School, Frankfurt am Main, Germany

In recent years Hagedorn states have been used to explain the physics close to the critical temperature within a hadron gas. Because of their large decay widths, these massive resonances lower η/s to near the AdS/CFT limit within the hadron gas phase. A comparison of the Hagedorn model to recent lattice results is made and it is found that for both $T_c = 176$ MeV and $T_c = 196$ MeV, the hadrons can reach chemical equilibrium almost immediately, well before the chemical freeze-out temperatures found in thermal fits for a hadron gas without Hagedorn states. In this paper we also observe the effects of Hagedorn states on the K^+/π^+ horn seen at AGS, SPS, and RHIC.

PACS: 25.75.-q

INTRODUCTION

As two heavy ions collide color neutral clusters are formed within which the number of particles per cluster increase. The clusters become so dense and begin to overlap so that it is impossible to distinguish quarks from one cluster from those in another, i.e., a percolation transition. The critical density for this is about $\epsilon \approx 1$ GeV/fm^3. Following the phase transition into Quark–Gluon Plasma, the interactions are dominated by quarks and gluons. Through gluon fusions, strange quarks can easily be reproduced. Eventually the QGP cools back into hadrons where the particle yields and ratios are measured.

If one only considers binary collisions, which react too slowly for strange particles to reach chemical equilibrium within the hadron gas phase, then it is clear that strange particle yields can only be explained through gluon fusion within QGP [1] and that the hadrons must exist in QGP already in full chemical equilibrium [2]. However, multimesonic collisions $n\pi \leftrightarrow X\bar{X}$ have been demonstrated to reach chemical equilibration for various (strange) antibaryons quickly at SPS [3, 4], although they are still not enough to explain the particle yields of exotic antibaryons at the higher energies at RHIC [5, 6]. In order to circumvent such longer time scales ~ 10 fm/c for a situation of a nearly baryon-free system with nearly as much antibaryons as baryons, it was then suggested by Braun-Munzinger, Stachel and Wetterich [7] that near T_c there exists an extra large particle density overpopulated with pions and kaons, which then drive the baryons/antibaryons into equilibrium by exactly such multimesonic collisions. But it is not clear how and why this overpopulation of pions and kaons should appear, and how the subsequent population of (anti)baryons would follow in accordance with a standard statistical hadron model: According to the mass action law the overpopulated matter of pions will result in an overpopulation of (anti)baryons. For such a large number of (anti)baryons it is difficult to get rid of them quickly enough in order to reach standard hadron equilibrium values before the chemical freeze-out [8].

Rather, understanding the rapid chemical equilibration is possible using Hagedorn states, heavy resonances that drive similar and more multihadronic reactions close to T_c, as shown in [8–12]. Close to T_c the matter is then a strongly interacting mixture of standard hadrons and such resonances. Using the Hagedorn states as potential and highly unstable catalysts, the standard hadrons can be populated reactions:

$$n\pi \leftrightarrow HS \leftrightarrow n'\pi + X\bar{X}, \tag{1}$$

where $X\bar{X}$ can be substituted with $p\bar{p}$, $K\bar{K}$, $\Lambda\bar{\Lambda}$, or $\Omega\bar{\Omega}$. The large masses of the decaying Hagedorn states open up the phase space for multiparticle decays.

In this note we will compare the particle ratios obtained by using reactions driven by Hagedorn states and those of the experiments at RHIC. We find that both strange and nonstrange particles match the experimental data well within the error bars. Furthermore, we are able to make estimates for the chemical equilibration time and find that they are very short, which implies that the hadrons can easily reach chemical equilibrium within an expanding, hadronic fireball and that hadrons do not need to be «born» into chemical equilibrium [10–12]. Hagedorn states thus provide a microscopic basis for understanding hadronization of deconfined matter to all hadronic particles.

Before starting with the details, we emphasize that Hagedorn states have become quite popular to understand the physics of strongly interacting matter close to the critical temperature: Hagedorn states have been shown to contribute to the physical description of a hadron gas close to T_c. The inclusion of Hagedorn states leads to a low η/s in the hadron gas phase [13], which nears the string theory bound $\eta/s = 1/(4\pi)$. Calculations of the trace anomaly including Hagedorn states also fit recent lattice results well and correctly describe the minimum of the speed of sound squared, c_s^2, near the phase transition found on the lattice [13]. Estimates for the bulk viscosity including Hagedorn states in the hadron gas phase indicate that the bulk viscosity, ζ/s, increases near T_c [13]. We also remark here that Hagedorn states can also explain the phase transition above the critical temperature and, depending on the intrinsic parameters, the order of the phase transition [14].

Because of the success of thermal models when fitting experimental data at RHIC, SPS, and AGS [15–21], a study was done on the effect of adding in the influence of Hagedorn states to the thermal models at RHIC energies [22,23]. It was found that not only does the addition of Hagedorn states improve the χ^2 of the fit but that the addition of Hagedorn states increases slightly the chemical freeze-out temperature. Due to the success of the implementation of Hagedorn states into other aspects of hadronic gas physics, we have decided to investigate the possible effects that Hagedorn states would have on the horn seen in the K^+/π^+ ratio [24,25]. A recent study has investigated the effects by adding in the decay of Hagedorn states into pions [26]. In this proceedings we will include the effects of Hagedorn states on all particles, not just the pions, in order to observe the horn. We find that the Hagedorn states do not contribute significantly to the horn.

1. SETUP

The basis of the Hagedorn spectrum is that there is an exponential mass increase along with a prefactor; i.e., the mass spectrum has the form: $f(m) \approx \mathrm{e}^{m/T_H}$ [27]. The exponential mass spectrum drives open the phase space, which allows for multimesonic decays to dominate

close to T_c (we assume $T_H \approx T_c$). We use the form

$$\rho = \int_{M_0}^{M} \frac{A}{[m^2 + m_r^2]^{5/4}} \exp\left(\frac{m}{T_H}\right) dm, \tag{2}$$

where $M_0 = 2$ GeV and $m_r^2 = 0.5$ GeV. We consider two different lattice results for T_c: $T_c = 196$ MeV [28,29] (the corresponding fit to the trace anomaly is then $A = 0.5$ GeV$^{3/2}$, $M = 12$ GeV, and $B = (340 \text{ MeV})^4$), which uses an almost physical pion mass, and $T_c = 176$ MeV [30] (the corresponding fit to the energy density leads to $A = 0.1$ GeV$^{3/2}$, $M = 12$ GeV, and $B = (300 \text{ MeV})^4$). Both are shown and discussed in [12]. Furthermore, we need to take into account the repulsive interactions and, thus, use volume corrections [12,13,31], which ensure that our model is thermodynamically consistent. Note that B is a free parameter based upon the idea of the MIT bag constant.

We need to consider the back reactions of multiple particles combining to form a Hagedorn state in order to preserve detailed balance. The rate equations for the Hagedorn resonances N_i, pions N_π, and the $X\bar{X}$ pair $N_{X\bar{X}}$, respectively, are given by

$$\dot{N}_i = \Gamma_{i,\pi}\left[N_i^{\rm eq}\sum_n B_{i,n}\left(\frac{N_\pi}{N_\pi^{\rm eq}}\right)^n - N_i\right] + \Gamma_{i,X\bar{X}}\left[N_i^{\rm eq}\left(\frac{N_\pi}{N_\pi^{\rm eq}}\right)^{\langle n_{i,x}\rangle}\left(\frac{N_{X\bar{X}}}{N_{X\bar{X}}^{\rm eq}}\right)^2 - N_i\right],$$

$$\dot{N}_\pi = \sum_i \Gamma_{i,\pi}\left[N_i\langle n_i\rangle - N_i^{\rm eq}\sum_n B_{i,n} n\left(\frac{N_\pi}{N_\pi^{\rm eq}}\right)^n\right] + \sum_i \Gamma_{i,X\bar{X}}\langle n_{i,x}\rangle\left[N_i - N_i^{\rm eq}\left(\frac{N_\pi}{N_\pi^{\rm eq}}\right)^{\langle n_{i,x}\rangle}\left(\frac{N_{X\bar{X}}}{N_{X\bar{X}}^{\rm eq}}\right)^2\right], \tag{3}$$

$$\dot{N}_{X\bar{X}} = \sum_i \Gamma_{i,X\bar{X}}\left[N_i - N_i^{\rm eq}\left(\frac{N_\pi}{N_\pi^{\rm eq}}\right)^{\langle n_{i,x}\rangle}\left(\frac{N_{X\bar{X}}}{N_{X\bar{X}}^{\rm eq}}\right)^2\right].$$

The decay widths for the ith resonance are $\Gamma_{i,\pi}$ and $\Gamma_{i,X\bar{X}}$, the branching ratio is $B_{i,n}$ (see below), and the average number of pions that each resonance will decay into is $\langle n_i\rangle$. The equilibrium values $N^{\rm eq}$ are both temperature- and chemical potential-dependent. However, here we set $\mu_b = 0$. Additionally, a discrete spectrum of Hagedorn states is considered, which is separated into mass bins of 100 MeV.

The branching ratios, $B_{i,n}$, are the probability that the ith Hagedorn state will decay into n pions where $\sum_n B_{i,n} = 1$ must always hold. We assume the branching ratios follow a Gaussian distribution for the reaction HS $\leftrightarrow n\pi$:

$$B_{i,n} \approx \frac{1}{\sigma_i\sqrt{2\pi}} \exp\left[-\frac{(n - \langle n_i\rangle)^2}{2\sigma_i^2}\right], \tag{4}$$

which has its peak centered at $\langle n_i\rangle \approx 3{-}34$ and the width of the distribution is $\sigma_i^2 \approx 0.8{-}510$ (see [12]). For the average number of pions when an $X\bar{X}$ pair is present, we again refer to the microcanonical model in [8,32] and find

$$\langle n_{i,x}\rangle = \left(\frac{2.7}{1.9}\right)(0.3 + 0.4m_i) \approx 2{-}7, \tag{5}$$

where m_i is in GeV. In this paper we do not consider a distribution but rather only the average number of pions when an $X\bar{X}$ pair is present. We assume that $\langle n_{i,x}\rangle = \langle n_{i,p}\rangle = \langle n_{i,k}\rangle = \langle n_{i,\Lambda}\rangle = \langle n_{i,\Omega}\rangle$ for when a kaon–antikaon pair, $\Lambda\bar{\Lambda}$, or $\Omega\bar{\Omega}$ pair is present.

The decays widths are defined as follows (see [12]):

$$\begin{aligned} \Gamma_i =& 0.15m_i - 0.0584 = 250 \text{ to } 1800 \text{ MeV}, \\ \Gamma_{i,X\bar{X}} &= \langle X_i\rangle \Gamma_i, \quad \Gamma_{i,\pi} = \Gamma_i - \Gamma_{i,X\bar{X}}. \end{aligned} \tag{6}$$

Γ_i is a linear fit extrapolated from the data in [33]. It is then separated into two parts, one for the reaction $\mathrm{HS} \leftrightarrow n\pi$, i.e., $\Gamma_{i,\pi}$, and one for the reaction $\mathrm{HS} \leftrightarrow n\pi + X\bar{X}$, i.e., $\Gamma_{i,X\bar{X}}$. The decay width $\Gamma_{i,X\bar{X}}$ is found by multiplying $\langle X_i\rangle$, which is the average X that a Hagedorn state of mass m will decay into, that is found from both microcanonical [8,32] and canonical models [12]. The large masses open up the phase space for such more special multiparticle decays. A detailed explanation is found in [12].

The equilibrium values are found using a statistical model [34], which includes 104 light or strange particles from the PDG [33]. Throughout this paper our initial conditions are the various fugacities at t_0 (at the point of the phase transition into the hadron gas phase) $\alpha \equiv \lambda_\pi(t_0)$, $\beta_i \equiv \lambda_i(t_0)$, and $\phi \equiv \lambda_{X\bar{X}}(t_0)$ which are chosen by holding the contribution to the total entropy from the Hagedorn states and pions constant, i.e., $s_{\mathrm{had}}(T_0,\alpha)V(t_0) + s_{\mathrm{HS}}(T_0,\beta_i)V(t_0) = s_{\mathrm{had+HS}}(T_0)V(t_0) = \mathrm{const}$ and the corresponding initial condition configurations we choose later can be seen in table (for further discussion, see [12]). In our model we do not just consider the direct number of hadrons but also the indirect number that comes from other resonances. For example, for pions we consider also the contribution from resonances such as ρ's, ω's, etc. The number of indirect hadrons can be calculated from the branching ratios for each individual species in the particle data book [33]. Moreover, there is also a contribution from the Hagedorn states to the total number of pions, kaons, and so on, as described in [10, 12]. Thus, the total number of «effective» pions can be described by

$$\tilde{N}_\pi = N_\pi + \sum_i N_i \langle n_i\rangle, \tag{7}$$

whereas the total number of «effective» p's, K's, Λ's, etc. (generalized as X) can be described by

$$\tilde{N}_X = N_X + \sum_i N_i \langle X_i\rangle. \tag{8}$$

Because the Hagedorn states are relevant only near T_c, the contribution of the Hagedorn states to the total particles numbers is only effected close to T_c.

Initial condition configurations

	$\alpha = \lambda_\pi(t_0)$	$\beta_i = \lambda_i(t_0)$	$\phi = \lambda_{X\bar{X}}(t_0)$
IC_1	1	1	0
IC_2	1	1	0.5
IC_3	1.1	0.5	0
IC_4	0.95	1.2	0

2. RESULTS: EXPANSION

In order to include the cooling of the fireball, we need to find a relationship between the temperature and the time, i.e., $T(t)$. To do this, we apply a Bjorken expansion for which the total entropy is held constant:

$$\text{const} = s(T)\,V(t) \sim \frac{S_\pi}{N_\pi}\int \frac{dN_\pi}{dy}dy, \tag{9}$$

where $s(T)$ is the entropy density of the hadron gas with volume corrections. The total number of pions in the 5% most central collisions, dN_π/dy, can be found from experimental results in [35]. Thus, our total pion number is $\sum\limits_i N_{\pi^i} = \int\limits_{-0.5}^{0.5}(dN_\pi/dy)dy = 874$. While for a gas of noninteracting Bose gas of massless pions $S_\pi/N_\pi = 3.6$, we do have a mass for our pions, so we must adjust S_π/N_π accordingly. In [36] it was shown that when the pions have a mass, the ratio changes and, therefore, the entropy per pion is close to $S_\pi/N_\pi \approx 5.5$, which is what we use here.

The effective volume at midrapidity can be parametrized as a function of time. We do this by using a Bjorken expansion and including accelerating radial flow. The volume term is then

$$V(t) = \pi\, ct\left(r_0 + v_0(t-t_0) + \frac{1}{2}a_0(t-t_0)^2\right)^2, \tag{10}$$

where the initial radius is $r_0(t_0) = 7.1$ fm for $T_H = 196$ and the corresponding $t_0^{(196)} \approx 2$ fm/c. For $T_H = 176$ we allow for a longer expansion before the hadron gas phase is reached and, thus, calculate the appropriate $t_0^{(176)}$ from the expansion starting at $T_H = 196$, which is $t_0^{(176)} \approx 4$ fm/c. We use $v_0 = 0.5$ and $a_0 = 0.025$ (see [12]).

Because the volume expansion depends on the entropy and the Hagedorn resonances contribute strongly to the entropy only close to the critical temperature (see [12]), the effects of the Hagedorn states must be taken into account with calculating the total particle yields otherwise the yields do not increase with the temperature (see [12] for further discussion). This is precisely what is done in Eqs. (7) and (8) because Hagedorn states also contribute strongly to the π's and $X\bar{X}$ pairs close to T_c.

Along with the expansion, we also must solve these rate equations, Eq. (3), numerically. We start with various initial conditions as seen in table and the initial temperature is the respective critical temperature and we stop at $T = 110$ MeV. A summary graph of all our results is shown in Fig. 1. The black error bars cover the range of error for the experimental data points from STAR and PHENIX. The points show the range in values for the initial conditions at a final expansion point with a temperature $T = 110$ MeV. We see in our graph that our freeze-out results match the experiments well and the initial conditions have little effect on the ratios, which implies that information from the QGP regarding multiplicities is washed out due to the rapid dynamics of Hagedorn states. A smaller β_i slows the equilibrium time slightly. However, as seen in Fig. 1, it still fits within the experimental values. Further discussion of the effects of our chosen decay widths can be found in [12], as well as individual results for those ratios within an expanding fireball. Furthermore, in [10] we showed that the initial conditions play almost no role whatsoever in K/π^+ and $(B+\bar{B})/\pi^+$, thus strengthening our argument that the dynamics are washed out following the QGP.

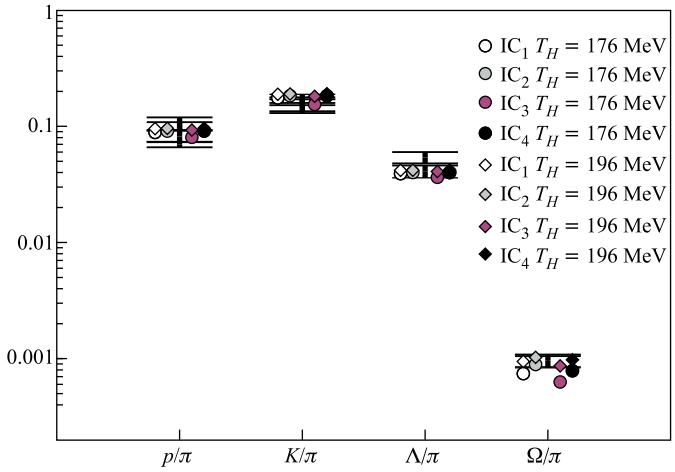

Fig. 1. Plot of the various ratios including all initial conditions defined in table. The points show the ratios at $T = 110$ MeV for the various initial conditions (circles are for $T_H = 176$ MeV and diamonds are for $T_H = 196$ MeV). The experimental results for STAR and PHENIX are shown by the black error bars

3. K^+/π^+ HORN

The K^+/π^+ ratio was first discussed in [24, 25] and has yet to be accurately explained using thermal models. However, it has been suggested that Hagedorn states could possibly be the explanation for the horn [26]. Using the $T_{\rm ch}$ and μ_b given in [19], we calculate the strange chemical potential, μ_s, with the conservation of strangeness

$$\frac{\sum\limits_i n_i S_i}{\sum\limits_i n_i B_i} = 0; \tag{11}$$

we are then able to calculate the corresponding K^+/π^+ at each experimental data point. At present we do not conserve charge (or rather isospin), however, we are currently working on a model that includes the electrical charge. We used data from RHIC, SPS, and AGS. The citations for the experimental data can all be found in [18, 19].

In Fig. 2 we have plotted the K^+/π^+ ratio versus $\sqrt{s_{NN}}$. The experimental data points are shown with the error bars, while our pure hadron gas is a dot. The two thermal model results with Hagedorn states are the square and star, which represent $T_H = 196$ MeV and $T_H = 176$ MeV, respectively. One can clearly see from the graph that there is almost no difference between the three different results. This is not surprising because at lower beam energies, the chemical freeze-out temperature is also lower. Around the peak of the horn the chemical freeze-out temperature ranges from $T = 124{-}160$ MeV, which means that most of the Hagedorn states have already died out even from the lower critical temperature of $T_H = 176$ MeV and have long since died out from $T_H = 196$ MeV. One can clearly see from the effects of the Hagedorn states on the total particle yields in Figs. 14 and 15 in [12] that at $T = 160$ MeV the Hagedorn states have almost no effect on the particle yields regardless of the T_H. If one were to lower the critical temperature closer to $T \approx 160$ MeV, then there

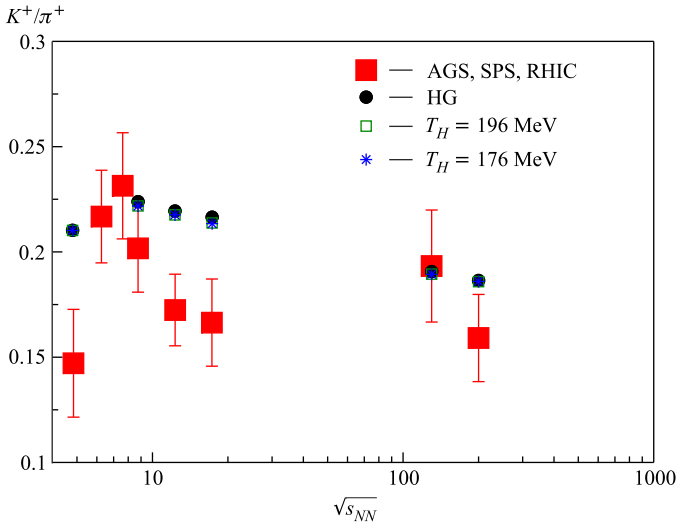

Fig. 2. Thermal model results for the K^+/π^+ ratio at various energies without Hagedorn states and with using two different Hagedorn temperatures: $T_H = 176$ MeV and $T_H = 196$ MeV. A comparison is shown to the data from AGS, SPS, and RHIC

might be a stronger influence of the Hagedorn states on the horn. In recent lattice calculations it has been suggested that the critical temperature might be lower [37], which we plan to look at in the future. Additionally, in our upcoming paper we will refit the results using a thermal model that conserves baryon number, charge, and strangeness.

CONCLUSION

In this paper we discussed the effects of Hagedorn states on the K^+/π^+ horn, which were found to be negligible. Because the K^+/π^+ horn is measured at lower beam energies than RHIC (and, hence, the typical temperatures are significantly below T_H, i.e., $T_{\rm ch} < 160$ MeV at the peak of the horn), it is not surprising that Hagedorn states do not play a role because Hagedorn states are highly suppressed far from the critical temperature. It is interesting to note that if recent lattice calculations are correct that exhibit a lower critical temperature region [37], then possibly the Hagedorn states could effect the K^+/π^+ horn, which we will attempt to study in a future paper. An attempt to look at Hagedorn states within this new lattice framework was shown in [38]. However, the repulsive interactions were not taken into account. As a future project we will create a thermal model that conserves baryon number, strangeness, and charge that looks specifically at the effects of Hagedorn states on thermal fits for energy ranges at AGS, SPS, and RHIC.

The Hagedorn states provide a mechanism for quick chemical equilibration times. Our model gives chemical equilibration times on the order of $\Delta\tau \approx 1{-}3$ fm/c. Furthermore, the particle ratios obtained from decays of Hagedorn states match the experimental values at RHIC very well, which leads to the conclusion that hadrons do not need to be born in chemical equilibrium. Rather a scenario of hadrons that reach chemical freeze-out shortly

after the critical temperature due to multimesonic reactions driven by Hagedorn states, is entirely plausible. We have shown that both strange (Λ's and K's) and nonstrange (π's and p's) hadrons can reach chemical equilibration by $T = 160$ MeV. Thus, it would be interesting to implement Hagedorn states into a transport approach such as UrQMD [39]. Such multiquark droplets are clearly recognized when looking at effective models of hadronization like the chromodielectric model [40]. Moreover, even multistrange baryons such as Ω's can reach chemical equilibrium in such a scenario. Our work indicates that the population and repopulation of potential Hagedorn states close to phase boundary can be the key source for a dynamical understanding of generating and chemically equilibrating the standard and measured hadrons. Hagedorn states thus can provide a microscopic basis for understanding hadronization of deconfined matter.

Acknowledgements. This work was supported by the Helmholtz International Center for FAIR within the framework of the LOEWE program (Landes-Offensive zur Entwicklung Wissenschaftlich-okonomischer Exzellenz) launched by the State of Hesse.

REFERENCES

1. *Koch P., Muller B., Rafelski J.* Strangeness in Relativistic Heavy Ion Collisions // Phys. Rep. 1986. V. 142. P. 167.
2. *Stock R.* The Parton to Hadron Phase Transition Observed in Pb + Pb Collisions at 158 GeV per Nucleon / Phys. Lett. B. 1999. V. 456. P. 277; arXiv:nucl-th/0703050.
3. *Rapp R., Shuryak E. V.* Resolving the Anti-Baryon Production Puzzle in High-Energy Heavy Ion Collisions // Phys. Rev. Lett. 2001. V. 86. P. 2980–2983; hep-ph/0008326.
4. *Greiner C.* Importance of Multi-Mesonic Fusion Processes on (Strange) Antibaryon Production // AIP Conf. Proc. 2003. V. 644. P. 337; Heavy Ion Phys. 2001. V. 14. P. 149;
   Greiner C., Leupold S. Antihyperon Production in Relativistic Heavy Ion Collision // J. Phys. G. 2001. V. 27. P. L95.
5. *Kapusta J. I., Shovkovy I.* Thermal Rates for Baryon and Anti-Baryon Production // Phys. Rev. C. 2003. V. 68. P. 014901;
   Kapusta J. I. Thermal Rates for Baryon and Anti-Baryon Production // J. Phys. G. 2004. V. 30. P. S351.
6. *Huovinen P., Kapusta J. I.* Rate Equation Network for Baryon Production in High Energy Nuclear Collisions // Phys. Rev. C. 2004. V. 69. P. 014902.
7. *Braun-Munzinger P., Stachel J., Wetterich C.* Chemical Freeze-out and the QCD Phase Transition Temperature // Phys. Lett. B. 2004. V. 596. P. 61.
8. *Greiner C. et al.* Chemical Equilibration due to Heavy Hagedorn States // J. Phys. G. 2005. V. 31. P. S725.
9. *Noronha-Hostler J., Greiner C., Shovkovy I. A.* Chemical Equilibration at the Hagedorn Temperature. nucl-th/0703079.
10. *Noronha-Hostler J., Greiner C., Shovkovy I. A.* Fast Equilibration of Hadrons in an Expanding Fireball // Phys. Rev. Lett. 2008. V. 100. P. 252301.
11. *Noronha-Hostler J. et al.* Chemical Equilibration and Transport Properties of Hadronic Matter near $T(c)$ // Nucl. Phys. A. 2009. V. 830. P. 745C–748C;
    Noronha-Hostler J., Greiner C., Shovkovy I. Chemical Equilibration of Baryons in an Expanding Fireball // Eur. Phys. J. ST. 2008. V. 155. P. 61; arXiv:nucl-th/0703079.

12. *Noronha-Hostler J. et al.* Dynamics of Chemical Equilibrium of Hadronic Matter Close to $T(c)$ // Phys. Rev. C. 2010. V. 81. P. 054909.

13. *Noronha-Hostler J., Noronha J., Greiner C.* Transport Coefficients of Hadronic Matter near T_c // Phys. Rev. Lett. 2009. V. 103. P. 172302.

14. *Zakout I., Greiner C., Schaffner-Bielich J.* The Order, Shape and Critical Point for the Quark–Gluon Plasma Phase Transition // Nucl. Phys. A. 2007. V. 781. P. 150;
Zakout I., Greiner C. The Thermodynamics for a Hadronic Gas of Fireballs with Internal Color Structures // Phys. Rev. C. 2008. V. 78. P. 034916.

15. *Braun-Munzinger P., Redlich K., Stachel J.* Particle Production in Heavy Ion Collisions. arXiv:nucl-th/0304013;
Braun-Munzinger P. et al. Thermal Equilibration and Expansion in Nucleus + Nucleus Collisions at the AGS // Phys. Lett. B. 1995. V. 344. P. 43; 1996. V. 365. P. 1;
Cleymans J. et al. Thermal Model Analysis of Particle Ratios at GSI Ni Ni Experiments Using Exact Strangeness Conservation // Phys. Rev. C. 1998. V. 57. P. 3319;
Cleymans J., Oeschler H., Redlich K. Influence of Impact Parameter on Thermal Description of Relativistic Heavy Ion Collisions at (1–2)A GeV // Phys. Rev. C. 1999. V. 59. P. 1663;
Averbeck R. et al. Neutral Pions and Eta Mesons as Probes of the Hadronic Fireball in Nucleus + Nucleus Collisions around $1A$ GeV // Phys. Rev. C. 2003. V. 67. P. 024903;
Braun-Munzinger P., Heppe I., Stachel J. Chemical Equilibration in Pb + Pb Collisions at the SPS // Phys. Lett. B. 1999. V. 465. P. 15;
Cleymans J. et al. Strangeness Production in Heavy Ion Collisions at Finite Baryon Number Density // Phys. Lett. B. 1990. V. 242. P. 111;
Cleymans J., Satz H. Thermal Hadron Production in High-Energy Heavy Ion Collisions // Z. Phys. C. 1993. V. 57. P. 135;
Becattini F., Gazdzicki M., Sollfrank J. On Chemical Equilibrium in Nuclear Collisions // Eur. Phys. J. C. 1998. V. 5. P. 143;
Becattini F. et al. Features of Particle Multiplicities and Strangeness Production in Central Heavy Ion Collisions between $1.7A$ GeV/c and $158A$ GeV/c // Phys. Rev. C. 2001. V. 64. P. 024901;
Torrieri G., Rafelski J. Strange Hadron Resonances as a Signature of Freeze-out Dynamics // Phys. Lett. B. 2001. V. 509. P. 239;
Torrieri G. et al. SHARE: Statistical Hadronization with Resonances // Comp. Phys. Commun. 2005. V. 167. P. 229;
Wheaton S., Cleymans J. THERMUS: A Thermal Model Package for ROOT // Comp. Phys. Commun. 2009. V. 180. P. 84;
Kisiel A. et al. THERMINATOR: Thermal Heavy-Ion Generator // Comp. Phys. Commun. 2006. V. 174. P. 669.

16. *Rafelski J., Kuznetsova I., Letessier J.* Strangeness and Threshold of Phase Changes // J. Phys. G. 2008. V. 35. P. 044011.

17. *Schenke B., Greiner C.* Statistical Description with Anisotropic Momentum Distributions for Hadron Production in Nucleus + Nucleus Collisions // J. Phys. G. 2004. V. 30. P. 597.

18. *Braun-Munzinger P. et al.* Hadron Production in Au + Au Collisions at RHIC // Phys. Lett. B. 2001. V. 518. P. 41;
Florkowski W., Broniowski W., Michalec M. Thermal Analysis of Particle Ratios and $p(T)$ Spectra at RHIC // Acta Phys. Polon. B. 2002. V. 33. P. 761;
Broniowski W., Florkowski W. Strange Particle Production at RHIC in a Single-Freeze-out Model // Phys. Rev. C. 2002. V. 65. P. 064905;
Kaneta M., Xu N. Centrality Dependence of Chemical Freeze-out in Au + Au Collisions at RHIC. arXiv:nucl-th/0405068;

Adams J. et al. (*STAR Collab.*). Experimental and Theoretical Challenges in the Search for the Quark–Gluon Plasma: The STAR Collaboration's Critical Assessment of the Evidence from RHIC Collisions // Nucl. Phys. A. 2005. V. 757. P. 102.

19. *Andronic A., Braun-Munzinger P., Stachel J.* Hadron Production in Central Nucleus + Nucleus Collisions at Chemical Freeze-Out // Nucl. Phys. A. 2006. V. 772. P. 167.
20. *Becattini F., Manninen J., Gazdzicki M.* Energy and System Size Dependence of Chemical Freeze-out in Relativistic Nuclear Collisions // Phys. Rev. C. 2006. V. 73. P. 044905; arXiv:hep-ph/0511092.
21. *Manninen J., Becattini F.* Chemical Freeze-out in Ultra-Relativistic Heavy Ion Collisions at $\sqrt{s_{NN}} = 130$ and 200 GeV // Phys. Rev. C. 2008. V. 78. P. 054901.
22. *Noronha-Hostler J. et al.* // Phys. Rev. C. (submitted); arXiv:0906.3960[nucl-th].
23. *Noronha-Hostler J., Noronha J., Greiner C.* Particle Ratios and the QCD Critical Temperature // J. Phys. G. 2010. V. 37. P. 094062; arXiv:nucl-th/1001.2610.
24. *Gazdzicki M. et al.* (*NA49 Collab.*). Report from NA49 // J. Phys. G. 2004. V. 30. P. S701; arXiv:nucl-ex/0403023.
25. *Alt C. et al.* (*NA49 Collab.*). Pion and Kaon Production in Central Pb + Pb Collisions at 20A and 30A GeV: Evidence for the Onset of Deconfinement // Phys. Rev. C. 2008. V. 77. P. 024903; arXiv:0710.0118 [nucl-ex].
26. *Andronic A., Braun-Munzinger P., Stachel J.* Thermal Hadron Production in Relativistic Nuclear Collisions: The Sigma Meson, the Horn, and the QCD Phase Transition // Phys. Lett. B. 2009. V. 673. P. 142; Erratum // Phys. Lett. B. 2009. V. 678. P. 516; arXiv:nucl-th/0812.1186.
27. *Hagedorn R.* Statistical Thermodynamics of Strong Interactions at High Energies. 3. Heavy-Pair (Quark) Production Rates // Nuovo Cim. Suppl. 1968. V. 6. P. 311; 1965. V. 3. P. 147.
28. *Cheng M. et al.* The QCD Equation of State with Almost Physical Quark Masses // Phys. Rev. D. 2008. V. 77. P. 014511.
29. *Bazavov A. et al.* Equation of State and QCD Transition at Finite Temperature. arXiv:hep-lat/0903.4379.
30. *Aoki Y. et al.* // JHEP. 2006. V. 0601. P. 089; Phys. Lett. B. 2006. V. 643. P. 46.
31. *Kapusta J. I., Olive K. A.* Thermodynamics of Hadrons: Delimiting the Temperature // Nucl. Phys. A. 1983. V. 408. P. 478.
32. *Liu F. M., Werner K., Aichelin J.* Comparison of Micro-Canonical and Canonical Hadronization // Phys. Rev. C. 2003. V. 68. P. 024905;
Liu F. M. et al. A Micro-Canonical Description of Hadron Production in Proton–Proton Collisions // J. Phys. G. 2004. V. 30. P. S589; Phys. Rev. C. 2004. V. 69. P. 054002.
33. *Eidelman S. et al.* // Phys. Lett. B. 2004. V. 592. P. 1.
34. *Spieles C., Stoecker H., Greiner C.* Hadron Production in Relativistic Nuclear Collisions: Thermal Hadron Source or Hadronizing Quark–Gluon Plasma? // Eur. Phys. J. C. 1998. V. 2. P. 351;
Greiner C. et al. The Creation of Strange Quark Matter Droplets as a Unique Signature for Quark–Gluon Plasma Formation in Relativistic Heavy Ion Collisions // Phys. Rev. D. 1988. V. 38. P. 2797;
Greiner C., Stoecker H. Distillation and Survival of Strange Quark Matter Droplets in Ultrarelativistic Heavy Ion Collisions // Phys. Rev. D. 1991. V. 44. P. 3517.
35. *Bearden I. G. et al.* (*BRAHMS Collab.*) // Phys. Rev. Lett. 2005. V. 94. P. 162301.
36. *Greiner C., Gong C., Muller B.* Some Remarks on Pion Condensation in Relativistic Heavy Ion Collisions // Phys. Lett. B. 1993. V. 316. P. 226.
37. *Borsanyi S. et al.* The QCD Equation of State with Dynamical Quarks. arXiv:hep-lat/1007.2580.

38. *Majumder A., Muller B.* Hadron Mass Spectrum from Lattice QCD. arXiv:hep-ph/1008.1747.

39. *Bass S. A. et al.* Microscopic Models for Ultrarelativistic Heavy Ion Collisions // Prog. Part. Nucl. Phys. 1998. V. 41. P. 255; 225;
Bleicher M. et al. Relativistic Hadron–Hadron Collisions in the Ultra-Relativistic Quantum Molecular Dynamics Model // J. Phys. G. 1999. V. 25. P. 1859.

40. *Martens G. et al.* Two- and Three-Body Color Flux Tubes in the Chromo-Dielectric Model // Phys. Rev. D. 2004. V. 70. P. 116010; arXiv:hep-ph/0407215.